Chemosphere 276 (2021) 130282

Contents lists available at ScienceDirect

Chemosphere

journal homepage: www.elsevier.com/locate/chemosphere

Gene co-expression network analysis reveals mechanisms underlying ozone-induced carbamazepine toxicity in zebrafish (*Danio rerio*) embryos

Johannes Pohl [a, *], Oksana Golovko [b], Gunnar Carlsson [a], Stefan Örn [a], Monika Schmitz [c], Ehsan Pashay Ahi [c, d]

[a] Department of Biomedical Sciences and Veterinary Public Health, Swedish University of Agricultural Sciences, Box 7028, 75007, Uppsala, Sweden
[b] Department of Aquatic Sciences and Assessment, Swedish University of Agricultural Sciences, Box 7050, 75007, Uppsala, Sweden
[c] Department of Organismal Biology, Comparative Physiology Section, Uppsala University, Norbyvägen 18A, 75236, Uppsala, Sweden
[d] Organismal and Evolutionary Biology Research Programme, University of Helsinki, Viikinkaari 9, 00014, Helsinki, Finland

HIGHLIGHTS

- Ozonation of carbamazepine potentiates its toxicity in zebrafish embryos.
- Cardiovascular and swim bladder development adversely affected.
- Toxicity mechanisms elucidated by gene co-expression network analysis.
- Upstream transcription factors identified, downregulation led to toxicity induction.
- Morphological and mechanistic data assembled in a putative AOP.

GRAPHICAL ABSTRACT

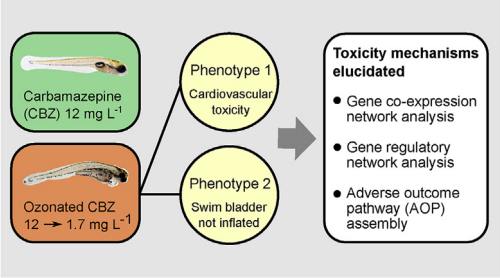

ARTICLE INFO

Article history:
Received 10 December 2020
Received in revised form
24 February 2021
Accepted 11 March 2021
Available online 14 March 2021

Handling Editor: Michael Bank

Keywords:
Toxicity mechanisms
Gene Co-Expression network analysis
Gene regulatory network analysis
Adverse outcome pathway

ABSTRACT

Sewage effluent ozonation can reduce concentrations of chemical pollutants including pharmaceutical residues. However, the formation of potentially toxic ozonation byproducts (OBPs) is a matter of concern. This study sought to elucidate toxicity mechanisms of ozonated carbamazepine (CBZ), an anti-epileptic drug frequently detected in sewage effluents and surface water, in zebrafish embryos (*Danio rerio*). Embryos were exposed to ozonated and non-ozonated CBZ from 3 h post-fertilization (hpf) until 144 hpf. Embryotoxicity endpoints (proportion of dead and malformed embryos) were assessed at 24, 48, and 144 hpf. Heart rate was recorded at 48 hpf. Exposure to ozonated CBZ gave rise to cardiovascular-related malformations and reduced heart rate. Moreover, embryo-larvae exposed to ozonated CBZ displayed a lack of swim bladder inflation. Hence, the expression patterns of CBZ target genes involved in cardiovascular and embryonal development were investigated through a stepwise gene co-expression analysis approach. Two co-expression networks and their upstream transcription regulators were identified, offering mechanistic explanations for the observed toxicity phenotypes. The study presents a novel application of gene co-expression analysis elucidating potential toxicity mechanisms of an ozonated pharmaceutical with environmental relevance. The resulting data was used to establish a putative adverse outcome pathway (AOP).

* Corresponding author. P.O Box 7028, 75007, Uppsala, Sweden.
E-mail address: johannespohl1989@gmail.com (J. Pohl).

https://doi.org/10.1016/j.chemosphere.2021.130282

1. Introduction

Pharmaceutical pollution in the environment is emerging as a topic of global concern (Fent et al., 2006; Hughes et al., 2013). Active pharmaceutical ingredients (APIs) and their metabolites are excreted in feces and/or urine following administration, ultimately ending up in sewage at concentration ranges of ng to μg per liter (Luo et al., 2014). Current conventional sewage treatment plants (STPs) are generally ineffective at removing APIs, leading to emissions to recipient waters and the terrestrial environment via sludge (Beek et al., 2016). Non-target organisms can be affected by API exposure, as a majority of drug-targets are evolutionarily conserved (Gunnarsson et al., 2008). Carbamazepine (CBZ) is one example of a persistent API commonly detected in the surface water environment (Björlenius et al., 2018). Several studies have indicated adverse effects of CBZ in aquatic organisms (da Silva Santos et al., 2018; Ferrari et al., 2003; Qiang et al., 2016; Yan et al., 2018). The pharmacological effects of CBZ include sodium-channel blocking properties, which lead to dampening of the central nervous system activity in the patient. These effects alleviate symptoms associated with e.g. epileptic seizures (Shorvon et al., 2017).

Advanced sewage treatment technologies, such as ozonation, have been assessed and implemented in e.g. Sweden to improve the removal of APIs (Antoniou et al., 2013; Baresel et al., 2016). While ozonation can reduce the concentrations of several API parent compounds, a multitude of intermediary transformation products are created in the treated effluent, some with toxic properties (Lee and Gunten, 2016). Ozonation of CBZ has been shown to induce its toxic potency in zebrafish (*Danio rerio*) embryo-larvae, manifested mainly as cardiovascular toxicity and arrested swim bladder maturation (Pohl et al., 2019). In the present work we sought to elucidate the potential mechanisms underlying the aforementioned toxicity phenotypes using a gene co-expression network analysis approach.

Gene co-expression network analysis is a method used to elucidate gene expression correlation patterns and their potential regulatory connections underlying complex biological processes (Serra et al., 2020). Furthermore, the identification of the upstream regulators of gene networks involved in specific phenotypical responses to a treatment allows for a mechanistic understanding (van Dam et al., 2018). The method has predominately been applied in the biomedical field to link gene co-expression networks to disease phenotypes (Liu et al., 2017; Yang et al., 2014; Zhang and Ng, 2016). The gene co-expression approach is also a powerful tool in the context of ecotoxicology (Ewald et al., 2020). This approach has been used to explore mechanisms underlying toxicity responses in e.g. zebrafish exposed to benzophenones (Meng et al., 2020). Furthermore, elucidating molecular mechanisms of toxicity is useful in the context of adverse outcome pathways (AOP). The AOP concept has been proposed as a framework to map out key events, from the molecular initiating event (i.e. toxicant-receptor binding) to the organism/population level, linking the exposure to an adverse effect (Ankley et al., 2010; LaLone et al., 2017).

Conventionally, high-throughput techniques providing expression profiles of a vast array of genes (e.g. transcriptomics) are used as the basis for gene co-expression network analysis. In the present study, however, we opted to use relatively inexpensive low-throughput techniques (i.e. qPCR) coupled with information collected from public databases. This approach aimed to deduce gene regulatory networks (GRN) underlying the ozonated CBZ toxicity in zebrafish embryo-larvae. Our previous study showed how ozonation of CBZ decreased the lowest observed effect concentration (LOEC) in all tested zebrafish embryo endpoints (Pohl et al., 2019). Thus, we hypothesized that ozonation of CBZ would exacerbate its transcriptional effects on developmentally important genes. The information gathered from the study was subsequently used to formulate a putative AOP of ozonated CBZ.

2. Materials and methods

2.1. Chemicals

CBZ (CAS number 298-46-4, purity ≥ 98%), CBZ internal standard (D_{10}), ethyl 3-amino-benzoate methanesulfonate salt (MS-222), liquid chromatography–mass spectrometry (LC/MS) grade acetonitrile, ethanol, methanol, isopropyl alcohol, chloroform, and ammonium acetate were purchased from MilliporeSigma. A Milli-Q Advantage ultrapure water purification system, a 0.22 μm Millipak express membrane filter, and an LC-Pak polishing unit (MilliporeSigma) were used to produce ultraclean water.

2.2. Chemical analysis

Water samples (V = 3 mL) were collected from the test solutions in triplicates in glass vials and stored in the freezer (- 20 °C) until chemical analysis. For chemical analysis, the samples were filtered using a regenerated cellulose syringe filter (0.22 mm pores). One milliliter of the filtered sample was spiked with 10 ng of internal standards of CBZ (D_{10}) per aliquot of sample. The analysis was carried out using liquid chromatography tandem-mass spectrometry (LC-MS/MS) with an LC system from Thermo Fisher Scientific and a triple-stage quadrupole MS/MS TSQ Quantiva (Thermo Fisher Scientific). An Acquity UPLC BEH-C18 column (100 mm x 2.1 i. d., 1.7 mm particle size from Waters Corporation) was used as an analytical column. Detailed information about instrumental analysis, sample preparation, and quality control is specified in our previous study (Pohl et al., 2020).

2.3. Bench-scale ozonation reactor set-up

The ozonation of CBZ in water solution was performed as specified in our previous study (Pohl et al., 2019). In brief, a CBZ stock solution (25 mg L^{-1} nominal concentration) was prepared in 250 mL aerated carbon-filtered tap water (pH: 8.41 ± 0.04, conductivity: 443 ± 18 mS cm^{-1}, alkalinity: 8 °dH, dissolved O_2: 97 ± 2%) and ozonated over 10 min (0.2 mg L^{-1} peak dissolved O_3) in room temperature (22 °C). Ozonation did not significantly affect the physiochemical properties. The dissolved O_3 concentration was measured by an LCK310 Ozone cuvette test (0.05–2 mg L^{-1} measurement range) in a DR 3900 spectrophotometer (Hach).

2.4. Zebrafish embryotoxicity tests and sampling

Zebrafish eggs were obtained from breeding groups of 10–15 laboratory-bred adult zebrafish. The eggs pooled and checked for fertilization success. Eggs from the spawning group displaying the highest fertilization success (>90%) were selected for exposure. The chorion was not removed from the embryos. Exposure to test solutions was initiated at approximately 3 h post-fertilization (hpf). All zebrafish embryo exposures were done at 26 °C and with a 12:12 h light/darkness photoperiod. Two parallel exposures using a single batch of fertilized zebrafish eggs were done to collect ample amounts of biological material for mRNA extraction (n = 8 per treatment, 40 embryos per pool) while maintaining sufficient replication (n = 24 per treatment, individual embryo exposure) for robust statistical analysis of toxicity phenotypes (Fig. 1).

The embryo pools destined for mRNA extraction were distributed in six-well plates (Costar) along with 4.5 mL test solution. Individually exposed embryos were transferred to 96-well plates (Costar) along with 200 μL test solution. The plates were sealed

with Parafilm M (Bemis NA, United States) in order to avoid evaporation. The embryos were exposed statically (i.e. no test solution change) until 48 hpf (mRNA extraction pools) or 144 hpf (toxicity phenotype screening) and subsequently euthanized by a high dose of MS-222 (1 g L^{-1}). Following euthanization, embryo pools exposed for mRNA extraction were rinsed in Milli-Q water, blotted dry, and collected in 300 μL RNA*Later* (ThermoFisher Scientific) for storage in fridge and freezer until mRNA extraction. The individually exposed embryos were checked for heart rate (beats per minute) at 48 hpf and incidence of death and malformations at 24, 48, and 144 hpf.

The measured CBZ concentration in the test solution was 12 mg L^{-1}. It is important to highlight that this concentration is 100–1000-fold higher than usually quantified in surface water (Björlenius et al., 2018). This concentration was selected as it corresponds to the LOEC of ozonated CBZ previously observed in zebrafish embryos (Pohl et al., 2019). Ozone treatment reduced the CBZ content by 86%, resulting in a CBZ concentration of 1.7 mg L^{-1} in the ozonated CBZ test solution.

2.5. Gene co-expression and regulatory network analysis

2.5.1. qPCR workflow

The total RNA was extracted using Trizol (Ambion), according to the manufacturer's protocol. In brief, the embryos were removed from RNA*Later* and homogenized with a fine syringe needle (25G Terumo needle and BD Plastipak 1 mL syringe) in 200 μl Trizol. Then, 40 μl of chloroform was added to each homogenized sample, followed by incubation, centrifugation, upper phase transfer steps with the addition of isopropyl alcohol. Samples were mixed rigorously, incubated at room temperature, and then centrifuged again to precipitate RNA pellets followed by three times washing with ice-cold 75% ethanol solution. The RNA pellets were solubilized in 10 μl of Nuclease-free water (Ambion) and treated with DNAse using the Turbo DNA-free kit (Ambion), according to the manufacturer's instructions. RNA quantity and quality were assessed spectrophotometrically using NanoDrop (ThermoFisher Scientific). Next, cDNA synthesis was carried out with 500 ng of RNA input from each sample, 0.5 μL of random primers (50 ng μl^{-1}) and 0.5 μl dNTP (10 nM), following incubation at 65 °C for 5 min. A mix containing 2 μl 5X First-Strand Buffer, 0.5 μl DTT (0.1 M), 0.5 μl RNase OUT (40 U/μl), and 0.5 μl Superscript III RT (200 U/μl) was prepared and added to each sample. The thermal profile of the reverse transcription was: 25 °C for 5 min, 50 °C for 50 min, and 70 °C for 15 min.

The qPCR primers for each gene were designed using sequences obtained from Blastn and zebrafish database (http://zfin.org) (Howe et al., 2013) and the CLC Genomic Workbench (CLC Bio). Exon/exon boundaries were specified based on the annotated *Danio rerio* genome in the Ensembl database (Flicek et al., 2012). Next, primers with short amplicon sizes (<200 bp) were designed using the Primer Express 3.0 software (Applied Biosystems). Dimerization and secondary structure formation were assessed through OligoAnalyzer 3.1 (Integrated DNA Technology). The primer sequences are presented in Supplementary Information Table S1 (candidate reference genes), Table S2 (cardiovascular-related target genes), and Table S3 (embryonic development target genes).

Relative gene expression data were procured using a MxPro-3000 PCR machine (Stratagene) and the MxPro software (Stratagene). For the qPCR, 1 μl diluted cDNA of each sample was mixed with 7.5 μl qPCR PowerUp SYBR Green Master mix (ThermoFischer Scientific), 0.3 μl forward and reverse primers (10 μM), and 6.2 μl RNA-free water. Each biological replicate was tested in two technical replicates for each gene following the sample maximization method to achieve an optimal experimental set-up (Hellemans et al., 2007). The qPCR program was followed by 50 °C for 2 min (1 cycle), 95 °C for 2 min (1 cycle), 95 °C for 15 s, and 62 °C for 1 min (40 cycles). A dissociation step (60 °C–95 °C) was conducted after the qPCR step, to verify product specificity. Primer efficiencies were determined calculated through standard curves of serial dilutions of pooled cDNA (random samples) and the following formula: $E = 10^{[-1/slope]}$. All primers had efficiencies exceeding or equal to 99% (Tables S1-S3).

For each gene, a biological replicate with the lowest expression level (highest Cq value) was used as calibrator value following the formula; $\Delta Cq_{\ target} - \Delta Cq_{\ calibrator}$, to calculate ΔΔCq values. The relative expression quantities (RQ) were calculated by $2^{-\Delta\Delta Cq}$ and their logarithmic values (fold changes) were used for statistical analysis (Pfaffl, 2001).

2.5.2. Reference gene validation

Identification of reference gene(s) with stable expression in every specific experimental condition is an essential step for the expression level normalization of target genes by qPCR (Ahi et al., 2017; Ahi and Sefc, 2018; Kubista et al., 2006). To find the most suitable reference genes, we applied three different algorithms commonly used for calculating the expression stabilities; BestKeeper (Pfaffl et al., 2004), NormFinder (Andersen et al., 2004), and geNorm (Vandesompele et al., 2002). BestKeeper utilizes two algorithms for reference gene ranking; one relies on the standard

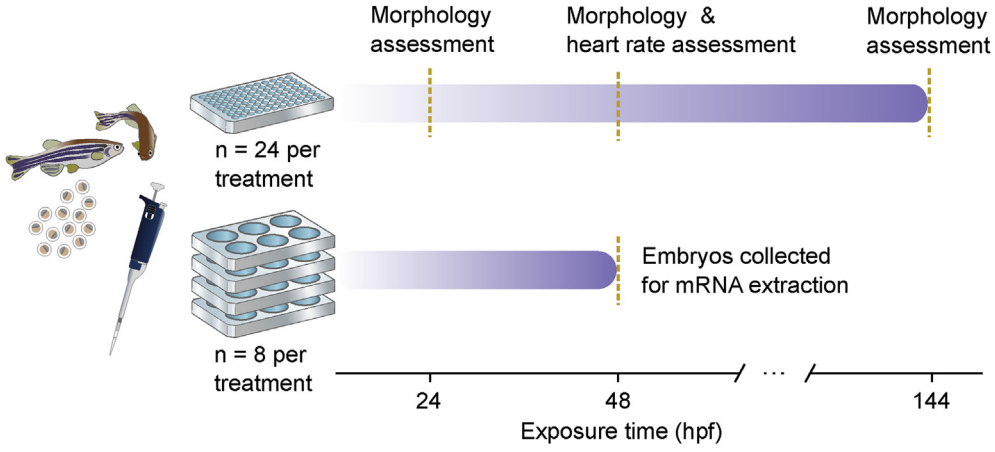

Fig. 1. Schematic representation of the zebrafish embryo exposure regime showing the two parallel exposures.

deviation of Cq values across all the samples and the other uses expression correlations or BestKeeper index (r) (Pfaffl et al., 2004). NormFinder finds the most stable genes by calculating expression stability values based on analysis of inter- and intra-group expression variation in expression (Andersen et al., 2004). On the other hand, geNorm calculates mean pairwise variations (M value) between each gene and the other candidates in a stepwise approach (Vandesompele et al., 2002). The ranking by each algorithm alone is not reliable unless similar results are observed across all of the algorithms (Ahi et al., 2019a, 2019b).

In this study, we assessed the expression levels of 8 candidate reference genes in zebrafish larva across the three experimental conditions. The expression of the candidate reference genes varied considerably. The highest expression (lowest Cq) was measured for *actb2* and *ef1a* at 17 Cq on average, while *b2m* displayed the lowest expression (highest Cq) at 30 Cq (Figure S1). According to all three algorithms (BestKeeper, geNorm, and Normfinder), *rplp13*, *tmem50,* and *ube2a* were consistently ranked as the most stably expressed genes (although the ranks were interchanging between the three genes), whereas *actb2* and *b2m* were ranked as the least stable candidates (Table S4). Therefore, the average expression level of *rplp13*, *tmem50*, and *ube2a* was used to normalize Cq values of target genes in each sample ($\Delta Cq_{\text{target}} = Cq_{\text{target}} - Cq_{\text{reference}}$).

2.5.3. Regulatory and gene co-expression network assembly

A step-wise iterative process was employed in order to construct gene co-expression networks and identify transcription factors (TFs) involved in producing the observed ozonated CBZ toxicity phenotypes in zebrafish embryo-larvae.

1. Expression profiles of two candidate CBZ target genes subsets related to cardiovascular (n = 11) and embryonic development (n = 12) were analyzed. Candidate gene selection was based on a transcriptomic study of zebrafish embryos exposed to CBZ (Hermsen et al., 2013).
2. A second set of co-expressed genes were selected according to a previously described gene regulatory network deduction approach (Ahi et al., 2015; Ahi and Sefc, 2018) using zebrafish co-expression data available at COXPRESdb (http://coxpresdb.jp/) version 7.0 (Obayashi et al., 2019). The evaluation yielded two subsets of co-expressed genes associated with cardiovascular (n = 12) and embryonic (n = 14) development which were subsequently analyzed by qPCR.
3. Two gene co-expression network modules were assembled based on the cardiovascular and embryonic development subsets. Upstream regulators were then predicted based on the co-expression modules. Motif enrichment on 4 kb upstream sequences (promoter and 5′-UTR) of the co-expression module genes was performed using MEME (Bailey et al., 2009). The enriched motifs were compared to position weight matrices (PWMs) obtained from the TRANSFAC database (Matys et al., 2003) using STAMP (Mahony and Benos, 2007) to identify potential TF binding sites.
4. Expression of the identified TFs upstream of the cardiovascular (n = 11) and embryonic development (n = 12) co-expression modules were analyzed by qPCR.

2.6. Statistical analysis

Analysis of variance (ANOVA) tests, followed by Tukey's honest significant difference (HSD) post hoc tests were used to compare treatment groups regarding continuous data (i.e. heart rate and mRNA expression). Categorical data (i.e. number of dead/malformed embryos) were tested with Bonferroni adjusted Fisher's exact tests. *P*-values lower than 0.05 were considered to indicate statistically significant deviations between treatment groups. The expression similarities between the genes across the treatment groups were assessed by pairwise Pearson correlation coefficients. R software (version 3.4.0) with the R-studio user interface (version 1.0.143) was used for statistical analysis and data visualization (R Core Team, 2019; RStudio Team, 2020).

3. Results and discussion

3.1. Zebrafish embryotoxicity assessment

Heart rate was reduced in embryos exposed to ozonated CBZ at 48 hpf (Fig. 2A). The morphological assessment showed that the ozonated CBZ exposure caused pericardial and/or non-inflated swim bladder phenotypes (Fig. 2C). The accumulated proportion of dead and malformed zebrafish embryo-larvae in the ozonated CBZ treatment was ~20% at 48 hpf and ~90% at 144 hpf (Fig. 2B). A similar trend of increasing proportions of dead and malformed embryo-larvae was also observed in the non-ozonated CBZ treatment, albeit non-significant (Fig. 2B). The observed responses corresponded well with our previous study on ozonated CBZ embryotoxicity (Pohl et al., 2019). The induced zebrafish embryotoxicity of CBZ following ozonation has been associated with the formation of ozonation byproducts, more specifically BQM and BQD (Pohl et al., 2020). Dissolved ozone has previously been shown not to produce any adverse effects in zebrafish embryos at concentrations used in the present study (Pohl et al., 2019).

The zebrafish embryonic heart development is initiated at the onset of gastrulation (~6 hpf), and by 48 hpf the embryonal cardiovascular system becomes operational (Collins and Stainier, 2016). Heart development is highly conserved among vertebrates, as more than 90% of human genes involved in heart formation and development have homologs in zebrafish (Shih et al., 2015). The swim bladder is a vital organ for buoyancy regulation in teleost fish species (Denton, 1961). The swim bladder develops in three phases; budding (~48 hpf), elongation (~80 hpf), and inflation (~100 hpf) (Winata et al., 2010). Larval fish displaying a lack of swim bladder inflation will ultimately fail to feed, leading to mortality. A proper cardiovascular function also carries importance for normal swim bladder development (Winata et al., 2009).

Interpretation of the mechanisms behind toxicity phenotypes could be challenging. For instance, pericardial edema formation may be associated with adverse effects in the kidney (Incardona and Scholz, 2016; Kramer-Zucker et al., 2005). It is therefore imperative to investigate the molecular mechanisms underlying the observed phenotypes to elucidate modes of action. As such, the present study moved on to analyze gene regulatory networks involved in zebrafish cardiovascular and embryonic development.

3.2. Gene co-expression network analysis

3.2.1. CBZ target genes involved in cardiovascular development

The mRNA expression of in total 34 genes associated with cardiovascular formation and function were analyzed by qPCR (Fig. 3). In the first batch of 11 candidate genes, *cavin4a*, *efemp2b*, *eya2*, *pfkma*, *pgm 1*, *ryr3*, and *uqcrc1* displayed significantly altered expression due to exposure to ozonated and/or non-ozonated CBZ as compared with the control treatment. Out of these genes, the mRNA expression of *cavin4a* was reduced in embryos exposed to ozonated CBZ, but not non-ozonated CBZ and the control group.

The *cavin4a* gene encodes cavin-4 (also known as muscle-restricted coiled-coil protein, or MURC), one of the four so-called cavins (cavin-1 through cavin-4) with important functions for the formation and function of caveolae, which are flask-shaped invaginations in the cell membrane (Hansen and Nichols, 2010). The

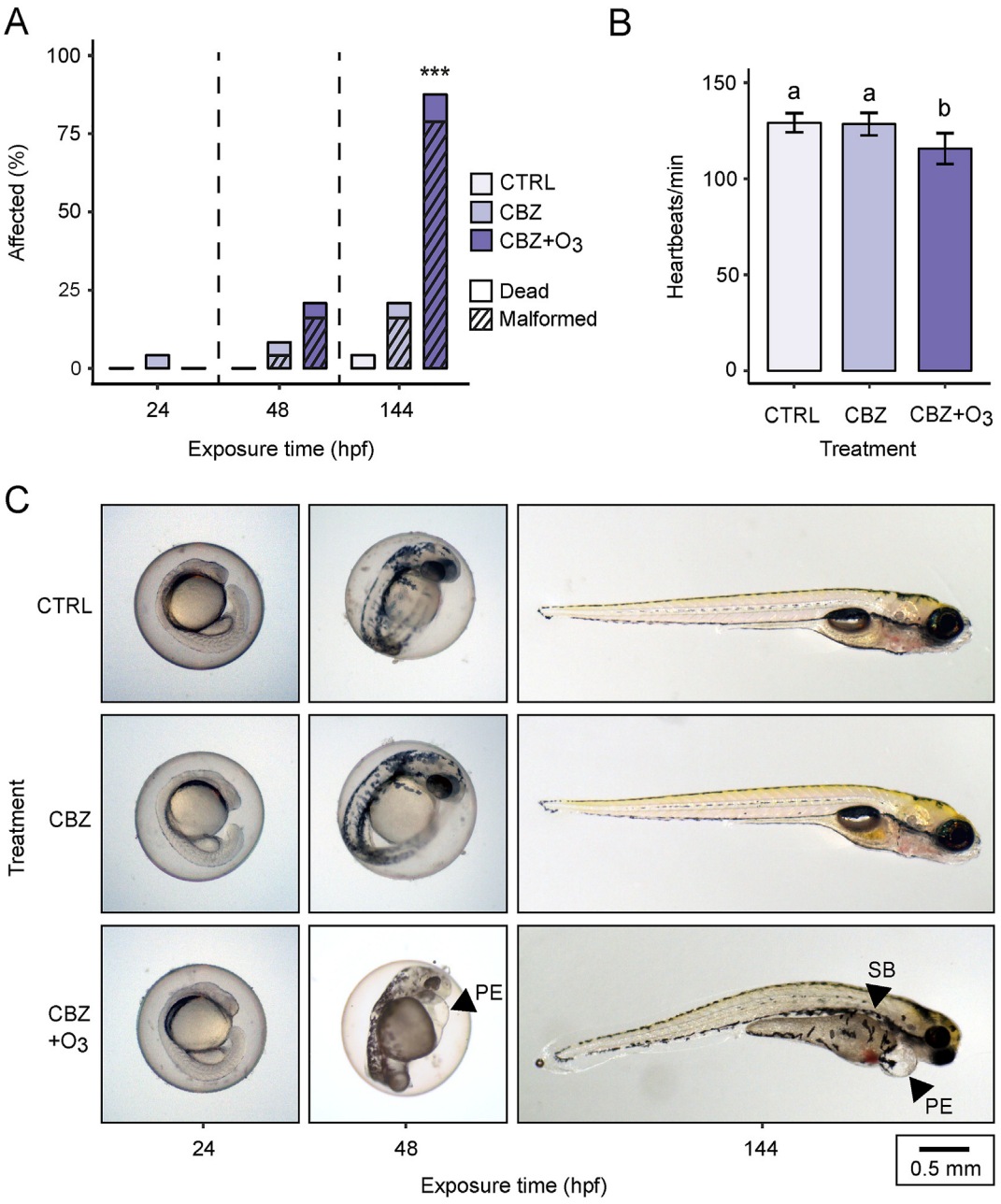

Fig. 2. (A) Embryo heart rate (heart beats per minute, mean ± sd) at 48 hpf (different letters indicate a significant deviation ($p < 0.05$, Tukey HSD test), (C) representative images of embryo-larvae in the three treatment groups at 24, 48, and 144 hpf with arrows indicating typical malformation (PE: pericardial edema, SB: lack of swim-bladder inflation), (D) proportion affected (dead and malformed) embryo-larvae at 24, 48, and 144 hpf (***: $p < 0.001$ in Bonferroni adjusted Fisher's exact test).

functions of caveolae are not fully known, but they have been proposed to have important cellular functions in cellular signaling pathways, cell endocytosis, lipid and cholesterol regulation, and mechanosensing (i.e. cellular response to physical manipulation) (Bastiani and Parton, 2010). Cavin4 is highly enriched in cardiac muscle plasma membranes (Bastiani et al., 2009; Ogata et al., 2008). Impaired *cavin* expression has been associated with adverse cardiovascular outcomes in both mice and zebrafish. (Lo et al., 2015; Naito et al., 2015). Zebrafish embryos injected with morpholinos silencing *cavin1a* expression gave rise to phenotypes displaying pericardial edemas (Lo et al., 2015). A similar phenotype was observed in embryos treated with ozonated CBZ in the present study (Fig. 2C). The impaired cardiovascular development in ozonated CBZ exposed zebrafish embryo-larvae may, therefore, be related to impacts on the caveolae functions and gene regulatory network(s) containing the *cavin4a* gene.

Since we sought to determine the gene regulatory network underlying the induced toxicity of CBZ post-ozonation, the COXPRESdb database was used to select 12 putatively *cavin4a* co-expressed genes for further qPCR expression analysis. Six of these genes (*actc1b*, *cavin4b*, *myl1*, *synpo2la*, *tnnc2*, and *tnnt3a*) showed significant down-regulation in the ozonated CBZ treatment group (Fig. 3). These genes encode proteins with important roles in skeletal (*actc1b* (Ojehomon et al., 2018; Shih et al., 2015), *myl1* (Burguière et al., 2011; Garcia de la serrana et al., 2018), and *tnnc2* (Sogah et al., 2010)), and cardiac (*synpo2la* (Beqqali et al., 2010)) muscle development. Interestingly, suppression of *tnnt3a* by morpholino knock-out can lead to a pericardial edema phenotype in

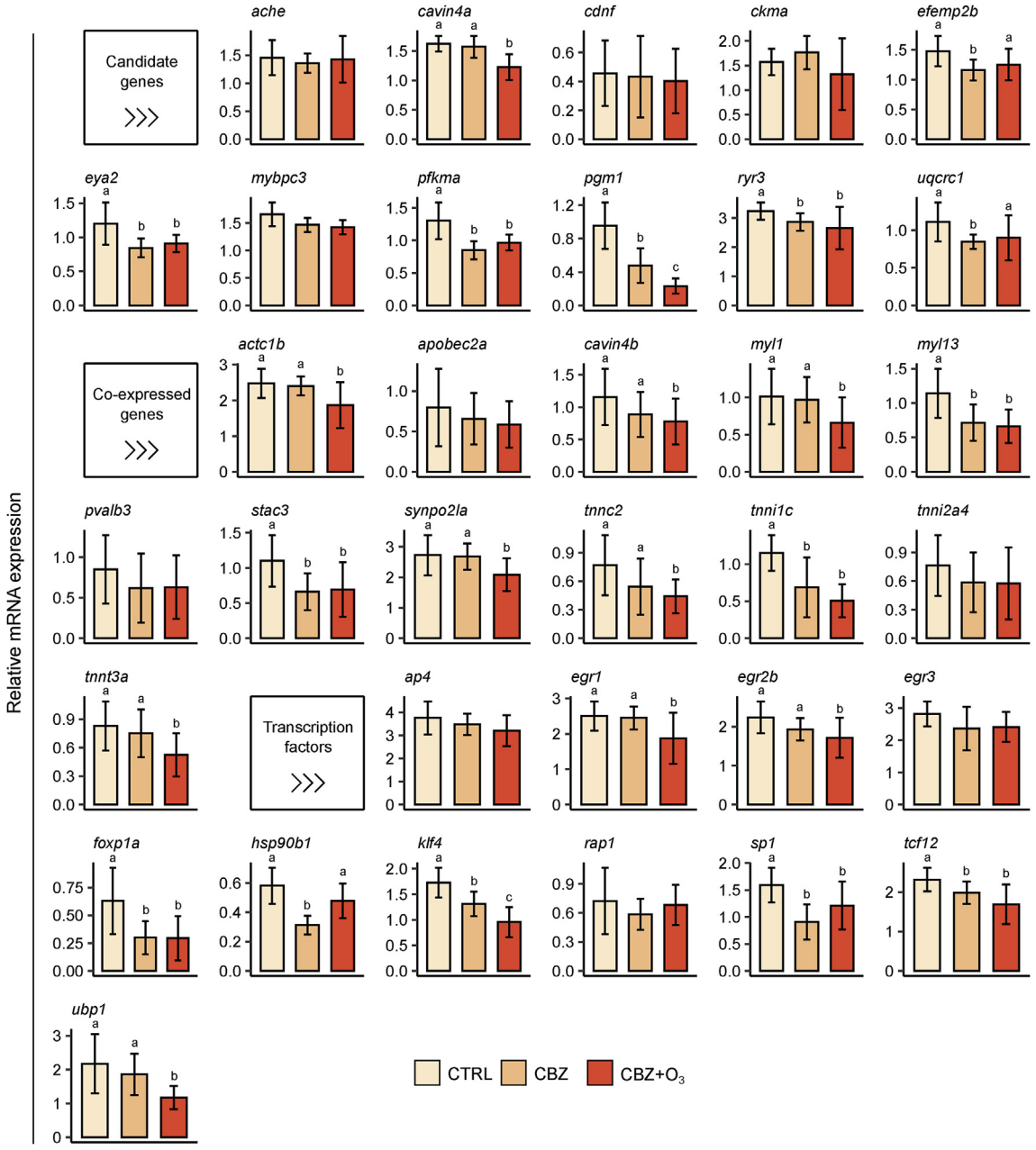

Fig. 3. Expression differences of selected candidate genes, *cavin4a* co-expressed genes, and TFs involved in cardiovascular formation and functions in the three treatment groups. Means and standard deviations of fold changes in expression of eight biological replicates are shown for each of the groups. Significant differences between treatments are indicated by different letters ($p < 0.05$, Tukeys HSD test).

zebrafish embryos, while not affecting heart rate (Ferrante et al., 2011).

Potential upstream regulators of the *cavin4a* co-expressed network were identified by searching TF binding sites in the upstream regulatory sequences. More than four motif sequences present in the regulatory sequences of all seven genes (Table S5). After parsing the motif sequences against known vertebrate TF binding sites, we found eleven sites matching the motifs (Table S5). Four of the 11 identified TFs, i.e. *egr1*, *egr2*, *klf4*, and *ubp1*, were down-regulated in embryos exposed to ozonated CBZ (Fig. 3). Two of these, *egr1* and *egr2*, encode members of the early growth response (EGR) family of C2H2-type zinc-finger proteins. These regulate a wide range of downstream genes that are involved in various biological processes such as the response to growth factors, DNA damage, ischemia, cell differentiation, and mitogenesis. Interestingly, dysregulation of both *egr1* and *egr2* is implicated in developmental and functional failures in the mammalian cardiovascular system such as cardiac hypertrophy and myocardial fibrosis (Buitrago et al., 2005; Hsu et al., 2013; Shen et al., 2019). However, the functions and developmental roles of *egr1* and *egr2* in zebrafish cardiovascular development are currently unknown. Kruppel like factor-4 gene or *klf4* also encodes a TF belonging to the zinc finger Kruppel family of TFs. *Klf4* is highly expressed in both myeloid cells and heart cells during zebrafish development, and its expression suppression in zebrafish embryos causes impairment in erythropoiesis and pericardial edema (Gardiner et al., 2007). In mammals, *Klf4* has a critical role in the normal function of cardiomyocytes and the progress of pathological cardiac development

as well as a significant decrease in cardiac output with increased lethality (Yoshida et al., 2010).

Upstream binding protein 1 gene, *ubp1*, is a TF with unknown function in zebrafish. However, in mice *upb1* is a major downstream target of microRNAs mediating oxidative stress during embryonic heart development (Dong et al., 2016). It should be noted that *ubp1* orthologues in mice and humans are highly expressed in the heart and aorta and it is implicated as a major factor determining blood pressure (Koutnikova et al., 2009).

3.2.2. CBZ target genes involved in embryonic development

A total of 38 genes related to zebrafish embryo development were analyzed by qPCR (Fig. 4). A subset of 12 candidate genes was initially assessed for mRNA expression. Out of these genes, *abca1a*, *abcc2*, *dct*, *pmela, tyr,* and *tyrp1b* displayed significantly reduced expression in both the CBZ and the ozonated CBZ treatments (Fig. 4). The genes *aox3* and *gch2* were down-regulated in the CBZ treatment group only. The expression of *dct, pmelb*, and *tyr* was significantly lower in the ozonated CBZ treatment group as compared to both CBZ and control (Fig. 4). This indicates that ozonation exacerbates the repressive effects of CBZ on specific genes involved in embryonic development.

The first gene, *dct*, dopachrome tautomerase or tyrosinase-related protein-2, catalyzes the conversion of L-dopachrome into 5,6-dihydroxyindole-2-carboxylic acid (DHICA) and involved in regulating eumelanin and phaeomelanin levels. In zebrafish, *dct* is developmentally expressed in the neural crest and has functions related to pigmentation (Kelsh et al., 2000; Potterf et al., 2001). The second gene, *pmelb*, premelanosome protein, encodes a melanocyte-specific transmembrane glycoprotein which is enriched in melanosomes (the melanin-producing organelles) and plays an essential role in the structural organization of premelanosomes. In zebrafish, *pmelb* is required for morphogenesis of photoreceptor cells and retinal pigmented epithelium, as well as the melanosome assembly process (Burgoyne et al., 2015). In cichlid fish, differential expression of *pmelb* has been associated with variations in skin pigmentation patterns (Ahi et al., 2020; Ahi and Sefc, 2017a, 2017b). The third gene, *tyr* or tyrosinase, encodes an enzyme with both tyrosine hydroxylase and dopa oxidase catalytic activities required for conversion of tyrosine to melanin. In zebrafish, *tyr* expression is essential for the formation of retinal pigmented epithelium, melanin biosynthesis, maturation of eye photoreceptor cell membrane, determination of eye size, normal visual behavior, and melanophores and iridophores stripe patterning (Haffter et al., 1996; Jao et al., 2013; Park et al., 2016). These observations indicate that ozonation of CBZ may lead to transcriptional repression of developmental genes with roles in neural crest cell lineages differentiation including neural, retinal cells, and pigment cells, whereas CBZ exposure alone did not cause the transcriptional effects.

The COXPRESdb database was again used to discover a subset of *dct*, *pmelb*, and *tyr* co-expressed genes. The method yielded 14 putatively co-expressed genes. Of these, six genes (*cax1*, *mlana*, *slc24a5*, *syngr1a*, *tnn,* and *zgc:91968*) showed a similar pattern of significant down-regulation in the ozonated CBZ treatment group compared to non-ozonated CBZ and controls (Fig. 4). Three genes, *slc2a11b*, *slc2a15b*, and *mitfa*, were down-regulated in both the ozonated and non-ozonated CBZ treatment group (Fig. 4). The gene *tyrp1a* was upregulated in both treatments compared to controls (Fig. 4). The *Cax1*, *Slc24a5*, and *Syngr1a* genes are primarily involved in zebrafish neuronal crest development, eye morphogenesis, and pigmentation (Lamason et al., 2005; Manohar et al., 2010; Thisse and Thisse, 2004; Yousaf et al., 2020). The role of *mlana* in zebrafish has not been investigated previously. In mice, *mlana* plays important role in pigmentation and is required for melanosome biogenesis and maintenance (Aydin et al., 2012). *Tnn*, Tenascin N or W, encodes an extracellular matrix protein that acts as a ligand and is involved in the neurite outgrowth and cell migration in hippocampus (Neidhardt et al., 2003). In mice, *Tnn* is reported to be involved in the development of kidney, bone, and smooth muscle as well, but its function in zebrafish development is still unclear (Scherberich et al., 2004). The product of the *zgc:91968* gene has unknown functions in vertebrates but is shown to be highly expressed in neural crest cells and melanophores during zebrafish development suggesting its potential role in neural crest cells-derived tissues (Farnsworth et al., 2020; Heffer et al., 2017).

Next, putative upstream regulators of the co-expressed network were identified. We found seven motif sequences present in the regulatory sequences of at least six out of the nine downstream genes displaying reduced expression in embryos exposed to ozonated CBZ (Table S6). After parsing the motif sequences against the known vertebrate TF binding sites, we identified altogether 12 TF binding sites matching the motifs (Table S6).

Next, we investigated the mRNA expression of the 12 predicted TFs and found that two, *tfe3b*, and *tfec* showed stronger expression reduction in embryos treated with ozonated CBZ (Fig. 4). Both *tfe3b* and *tfec* have the same binding site on the regulatory sequences of their target genes (i.e. the TFE binding site), and in addition to them, three other TFs including *tfe3a*, *tfeb,* and *mitf* also bind to the same site (Rehli et al., 1999). All these genes are members of the microphthalmia-TFE (MiT) subfamily of basic helix-loop-helix leucine zipper (bHLH-ZIP) TFs implicated in the regulation of tissue-specific gene expression in several cell lineages. The functional domains in these TFs as well as their binding site sequence appears to be highly conserved across evolutionary distant animals (Rehli et al., 1999). In zebrafish embryos, the expression of *tfe3b* has been observed in a range of tissues including lens placode, the mid/hindbrain boundary, optic epithelium, pharyngeal arches, and the pectoral fins (Lister et al., 2011). Further, *tfec* expression at the early stages of development has been identified in cranial neural crest cells and retinal pigment epithelium, and is later at the larval stage mainly seen in the dorsal part of the head, eye, and swim bladder (Lister et al., 2011). Interestingly, swim bladder inflation is arrested in zebrafish embryos mutants with silenced *tfec* expression (Mahony et al., 2016; Petratou et al., 2019). The suppression of *tfec* observed in zebrafish embryo-larvae exposed to ozonated CBZ could therefore be associated with the observed lack of swim bladder inflation in the present study.

3.2.3. Gene regulatory networks and putative AOP assembly

Pearson's correlation analyses revealed significant positive expression correlations between the cardiovascular (Fig. 5A) and embryonic (Fig. 5B) development genes and their respective TFs. These findings suggest the potential inductive transcriptional regulatory role of the TFs on the downstream co-expressed gene networks, by which their reduced expression after exposure to ozonated CBZ leads to down-regulation of their respective downstream gene network. A putative AOP illustrating the potential key molecular mechanisms underlying ozonated CBZ toxicity phenotypes was populated by the information gathered within the respective GRNs (Fig. 5C).

The observed toxicity phenotypes may lead to reduced embryo-larval survival and subsequent population effects. Arrested swim bladder inflation, while being a sub-lethal effect, causes reduced swimming performance which can affect feeding and other natural behaviors adversely (Villeneuve et al., 2014). Further, abnormal cardiovascular function during embryo-larval development could lead to reduced viability at later life stages (Incardona and Scholz, 2017). It is important to point out that the two observed toxicity phenotypes may have additional mechanistic explanations. For

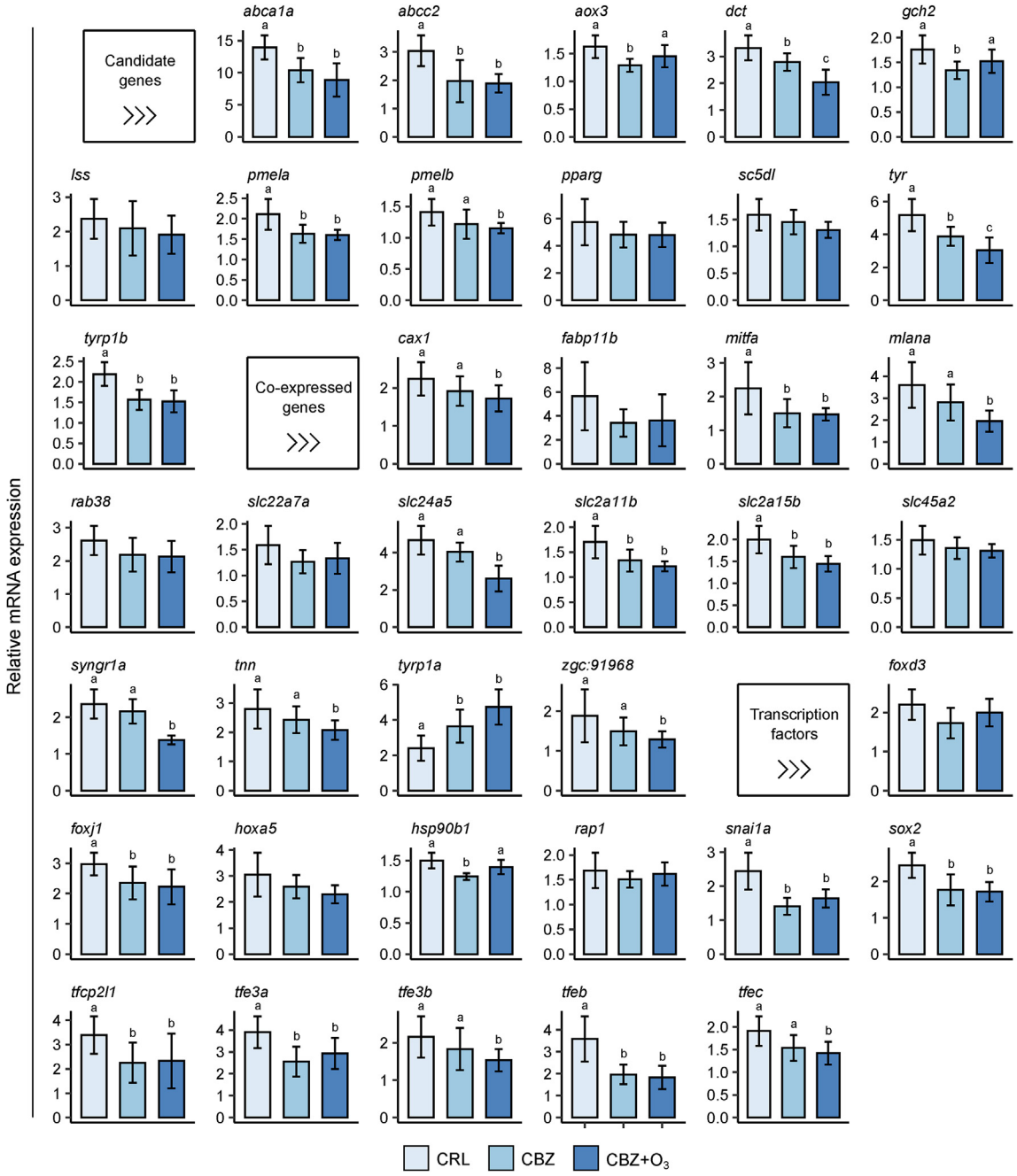

Fig. 4. Expression differences of selected candidate genes; *dct*, *pmelb,* and *tyr* co-expressed genes; and TFs involved in zebrafish embryonal development the three treatment groups. Means and standard deviations of fold changes in expression of eight biological replicates are shown for each of the groups. Significant differences between treatments are indicated by different letters ($p < 0.05$, Tukeys HSD test).

instance, the co-expression network associated with TFs *tf3b* and *tfec* (Fig. 5B) may also contribute to the cardiotoxicity phenotype since e.g. neural crest cells carry importance for zebrafish heart development (Cavanaugh et al., 2015).

4. Conclusions

The formation of toxic OBPs is problematic in the context of sewage effluent ozonation. The present work investigated mechanisms of ozone-induced CBZ toxicity (cardiovascular toxicity and/or lack of swim bladder inflation) in zebrafish embryo-larvae using a gene co-expression and regulatory network approach. Two gene co-expression network modules, and their associated upstream TFs, were identified. The first co-expression network module was populated by genes mainly involved in heart formation and functions, i.e. *cavin4a*, *cavin4b*, *actc1b*, *myl1*, *synpo2la*, *tnnc2*, and *tnnt3a*. These genes were down-regulated in embryo-larvae exposed to ozonated CBZ due to suppressed expression of the TFs *tfe3b* and *tfec*. The second co-expression network module consisted of genes (*dct*, *tyr*, *pmelb*, *cax1*, *mlana*, *slc24a5*, *syngr1a*, *tnn*, and *zgc:91968*) with important functions for pigmentation, neural crest, and swim bladder inflation. The expression of the upstream TFs *egr1, egr2, klf4,* and *ubp1* was suppressed leading to down-regulation of the gene co-expression network module. All toxicity and mechanistic

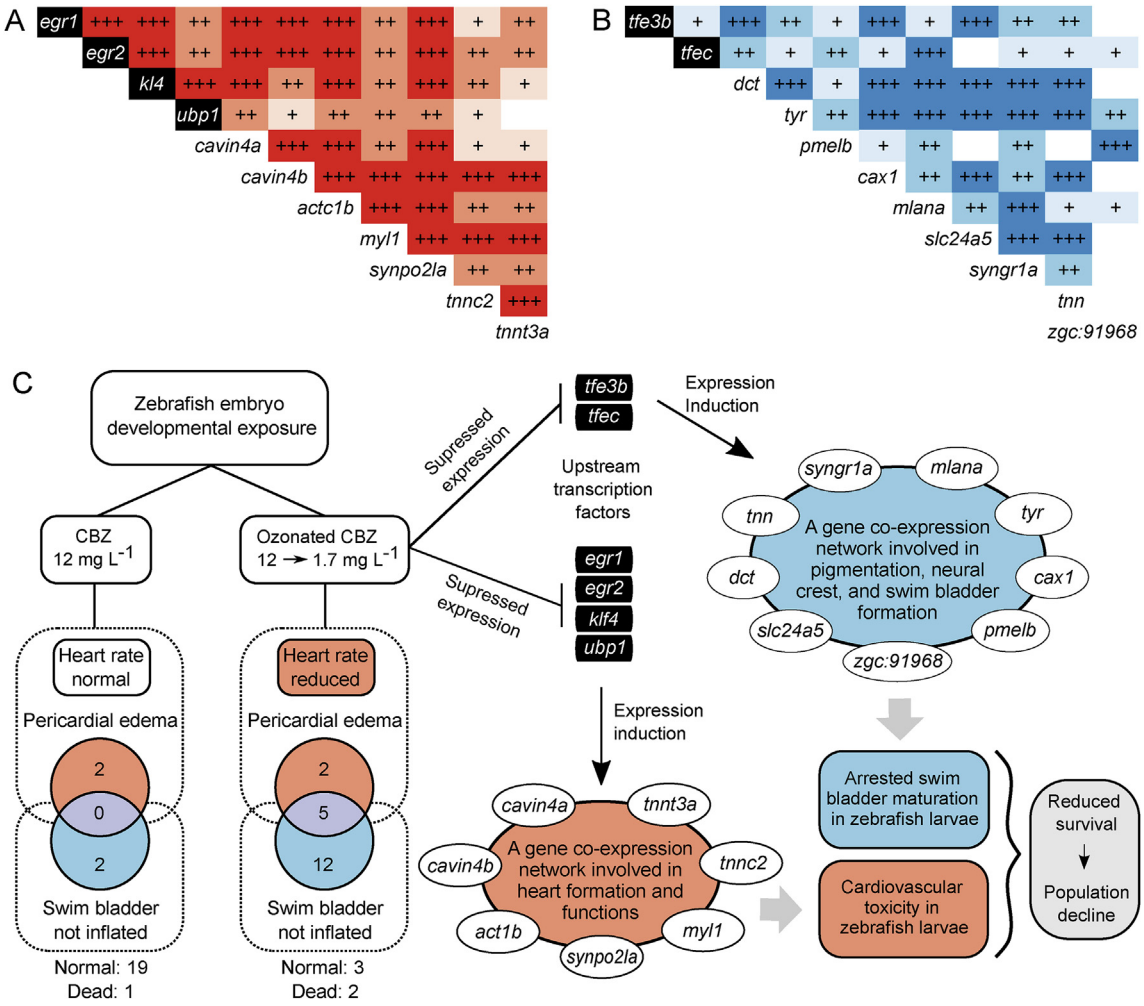

Fig. 5. Pairwise expression correlations between the members of the cardiovascular (A) and embryonic (B) developmental co-expression networks and their upstream regulators in zebrafish larvae. The plus signs indicate positive Pearson correlation coefficients, and 1 to 3 signs represent significant levels of $p < 0.05$, $p < 0.01$ and $p < 0.001$. (C) A schematic AOP illustration of the investigated mechanisms underlying ozonated CBZ toxicity phenotypes.

data collected throughout the study was organized and visualized in an AOP. The assembled AOP could be used as a starting point to further explore ozone-induced CBZ toxicity mechanisms. Additional information, such as the molecular initiating events leading to TF suppression, is important to collect in order to expand the AOP framework.

In sum, the present study showcased how qPCR gene expression techniques, informed by public databases, can be successfully applied to mechanistic inquiries of environmentally relevant contaminants and complex mixtures.

Credit

Johannes Pohl: Conceptualization, Funding acquisition, Writing – original draft, Methodology, Investigation, Formal analysis, Software, Visualization Oksana Golovko: Investigation, Methodology, Writing – review & editing Gunnar Carlsson: Resources, Writing – review & editing Stefan Örn: Resources, Writing – review & editing Monica Schmitz: Resources Ehsan Pashay Ahi: Conceptualization, Funding acquisition, Methodology, Investigation, Formal analysis, Visualization, Formal analysis, Writing – review & editing

Declaration of competing interest

The authors declare that they have no known competing financial interests or personal relationships that could have appeared to influence the work reported in this paper.

Acknowledgements

The study was made possible by a grant provided by the Centre for Reproductive Biology in Uppsala (CRU).

Appendix A. Supplementary data

Supplementary data to this article can be found online at https://doi.org/10.1016/j.chemosphere.2021.130282.

References

Ahi, E.P., Lecaudey, L.A., Ziegelbecker, A., Steiner, O., Glabonjat, R., Goessler, W., Hois, V., Wagner, C., Lass, A., Sefc, K.M., 2020. Comparative transcriptomics reveals candidate carotenoid color genes in an East African cichlid fish. BMC Genom. 21, 54. https://doi.org/10.1186/s12864-020-6473-8.

Ahi, E.P., Richter, F., Lecaudey, L.A., Sefc, K.M., 2019a. Gene expression profiling suggests differences in molecular mechanisms of fin elongation between cichlid species. Sci. Rep. 9, 9052. https://doi.org/10.1038/s41598-019-45599-w.

Ahi, E.P., Richter, F., Sefc, K.M., 2017. A gene expression study of ornamental fin

shape in Neolamprologus brichardi , an African cichlid species. Sci. Rep. 7, 17398. https://doi.org/10.1038/s41598-017-17778-0.
Ahi, E.P., Sefc, K.M., 2018. Towards a gene regulatory network shaping the fins of the Princess cichlid. Sci. Rep. 8, 9602. https://doi.org/10.1038/s41598-018-27977-y.
Ahi, E.P., Sefc, K.M., 2017a. A gene expression study of dorso-ventrally restricted pigment pattern in adult fins of Neolamprologus meeli, an African cichlid species. PeerJ 5, e2843. https://doi.org/10.7717/peerj.2843.
Ahi, E.P., Sefc, K.M., 2017b. Anterior-posterior gene expression differences in three Lake Malawi cichlid fishes with variation in body stripe orientation. PeerJ 5, e4080. https://doi.org/10.7717/peerj.4080.
Ahi, E.P., Singh, P., Duenser, A., Gessl, W., Sturmbauer, C., 2019b. Divergence in larval jaw gene expression reflects differential trophic adaptation in haplochromine cichlids prior to foraging. BMC Evol. Biol. 19, 150. https://doi.org/10.1186/s12862-019-1483-3.
Ahi, E.P., Steinhäuser, S.S., Pálsson, A., Franzdóttir, S.R., Snorrason, S.S., Maier, V.H., Jónsson, Z.O., 2015. Differential expression of the aryl hydrocarbon receptor pathway associates with craniofacial polymorphism in sympatric Arctic charr. EvoDevo 6, 27. https://doi.org/10.1186/s13227-015-0022-6.
Andersen, C.L., Jensen, J.L., Ørntoft, T.F., 2004. Normalization of real-time quantitative reverse transcription-PCR data: a model-based variance estimation approach to identify genes suited for normalization, applied to bladder and colon cancer data sets. Canc. Res. 64, 5245–5250. https://doi.org/10.1158/0008-5472.CAN-04-0496.
Ankley, G.T., Bennett, R.S., Erickson, R.J., Hoff, D.J., Hornung, M.W., Johnson, R.D., Mount, D.R., Nichols, J.W., Russom, C.L., Schmieder, P.K., Serrrano, J.A., Tietge, J.E., Villeneuve, D.L., 2010. Adverse outcome pathways: a conceptual framework to support ecotoxicology research and risk assessment. Environ. Toxicol. Chem. 29, 730–741. https://doi.org/10.1002/etc.34.
Antoniou, M.G., Hey, G., Rodríguez Vega, S., Spiliotopoulou, A., Fick, J., Tysklind, M., la Cour Jansen, J., Andersen, H.R., 2013. Required ozone doses for removing pharmaceuticals from wastewater effluents. Sci. Total Environ. 456–457, 42–49. https://doi.org/10.1016/j.scitotenv.2013.03.072.
Aydin, I.T., Hummler, E., Smit, N.P.M., Beermann, F., 2012. Coat color dilution in mice because of inactivation of the melanoma antigen MART-1. Pigment Cell Melanoma Res 25, 37–46. https://doi.org/10.1111/j.1755-148X.2011.00910.x.
Bailey, T.L., Boden, M., Buske, F.A., Frith, M., Grant, C.E., Clementi, L., Ren, J., Li, W.W., Noble, W.S., 2009. Meme suite: tools for motif discovery and searching. Nucleic Acids Res. 37, 202–208. https://doi.org/10.1093/nar/gkp335.
Baresel, C., Malmborg, J., Ek, M., Sehlén, R., 2016. Removal of pharmaceutical residues using ozonation as intermediate process step at Linköping WWTP, Sweden. Water Sci. Technol. 73, 2017–2024. https://doi.org/10.2166/wst.2016.045.
Bastiani, M., Liu, L., Hill, M.M., Jedrychowski, M.P., Nixon, S.J., Lo, H.P., Abankwa, D., Luetterforst, R., Fernandez-Rojo, M., Breen, M.R., Gygi, S.P., Vinten, J., Walser, P.J., North, K.N., Hancock, J.F., Pilch, P.F., Parton, R.G., 2009. MURC/Cavin-4 and cavin family members form tissue-specific caveolar complexes. J. Cell Biol. 185, 1259–1273. https://doi.org/10.1083/jcb.200903053.
Bastiani, M., Parton, R.G., 2010. Caveolae at a glance. J. Cell Sci. 123, 3831–3836. https://doi.org/10.1242/jcs.070102.
Beek, T., , aus der, Weber, F.A., Bergmann, A., Hickmann, S., Ebert, I., Hein, A., Küster, A., 2016. Pharmaceuticals in the environment—global occurrences and perspectives. Environ. Toxicol. Chem. 35, 823–835. https://doi.org/10.1002/etc.3339.
Beqqali, A., Monshouwer-Kloots, J., Monteiro, R., Welling, M., Bakkers, J., Ehler, E., Verkleij, A., Mummery, C., Passier, R., 2010. CHAP is a newly identified Z-disc protein essential for heart and skeletal muscle function. J. Cell Sci. 123, 1141–1150. https://doi.org/10.1242/jcs.063859.
Björlenius, B., Ripszám, M., Haglund, P., Lindberg, R.H., Tysklind, M., Fick, J., 2018. Pharmaceutical residues are widespread in Baltic Sea coastal and offshore waters – screening for pharmaceuticals and modelling of environmental concentrations of carbamazepine. Sci. Total Environ. 633, 1496–1509. https://doi.org/10.1016/j.scitotenv.2018.03.276.
Buitrago, M., Lorenz, K., Maass, A.H., Oberdorf-Maass, S., Keller, U., Schmitteckert, E.M., Ivashchenko, Y., Lohse, M.J., Engelhardt, S., 2005. The transcriptional repressor Nab 1 is a specific regulator of pathological cardiac hypertrophy. Nat. Med. 11, 837–844. https://doi.org/10.1038/nm1272.
Burgoyne, T., O'Connor, M.N., Seabra, M.C., Cutler, D.F., Futter, C.E., 2015. Regulation of melanosome number, shape and movement in the zebrafish retinal pigment epithelium by OA1 and PMEL. J. Cell Sci. 128, 1400–1407. https://doi.org/10.1242/jcs.164400.
Burguière, A.C., Nord, H., Hofsten, J. von, 2011. Alkali-like myosin light chain-1 (myl1) is an early marker for differentiating fast muscle cells in zebrafish. Dev. Dynam. 240, 1856–1863. https://doi.org/10.1002/dvdy.22677.
Cavanaugh, A.M., Huang, J., Chen, J.-N., 2015. Two developmentally distinct populations of neural crest cells contribute to the zebrafish heart. Dev. Biol. 404, 103–112. https://doi.org/10.1016/j.ydbio.2015.06.002.
Collins, M.M., Stainier, D.Y.R., 2016. Chapter twenty-five - organ function as a modulator of organ formation: lessons from zebrafish. In: Wassarman, P.M. (Ed.), Current Topics in Developmental Biology, Essays on Developmental Biology, Part B. Academic Press, pp. 417–433. https://doi.org/10.1016/bs.ctdb.2015.10.017.
da Silva Santos, N., Oliveira, R., Lisboa, C.A., Mona e Pinto, J., Sousa-Moura, D., Camargo, N.S., Perillo, V., Oliveira, M., Grisolia, C.K., Domingues, I., 2018. Chronic effects of carbamazepine on zebrafish: behavioral, reproductive and biochemical endpoints. Ecotoxicol. Environ. Saf. 164, 297–304. https://doi.org/10.1016/j.ecoenv.2018.08.015.
Denton, E.J., 1961. 6 - the buoyancy of fish and cephalopods. Prog. Biophys. Biophys. Chem. 11, 177–234. https://doi.org/10.1016/S0096-4174(18)30212-9.
Dong, D., Zhang, Y., Reece, E.A., Wang, L., Harman, C.R., Yang, P., 2016. microRNA expression profiling and functional annotation analysis of their targets modulated by oxidative stress during embryonic heart development in diabetic mice. Reprod. Toxicol. 65, 365–374. https://doi.org/10.1016/j.reprotox.2016.09.007.
Ewald, J.D., Soufan, O., Crump, D., Hecker, M., Xia, J., Basu, N., 2020. EcoToxModules: custom gene sets to organize and analyze toxicogenomics data from ecological species. Environ. Sci. Technol. 54, 4376–4387. https://doi.org/10.1021/acs.est.9b06607.
Farnsworth, D.R., Saunders, L.M., Miller, A.C., 2020. A single-cell transcriptome atlas for zebrafish development. Dev. Biol. 459, 100–108. https://doi.org/10.1016/j.ydbio.2019.11.008.
Fent, K., Weston, A.A., Caminada, D., 2006. Ecotoxicology of human pharmaceuticals. Aquat. Toxicol. 76, 122–159. https://doi.org/10.1016/j.aquatox.2005.09.009.
Ferrante, M.I., Kiff, R.M., Goulding, D.A., Stemple, D.L., 2011. Troponin T is essential for sarcomere assembly in zebrafish skeletal muscle. J. Cell Sci. 124, 565–577. https://doi.org/10.1242/jcs.071274.
Ferrari, B., Paxéus, N., Giudice, R.L., Pollio, A., Garric, J., 2003. Ecotoxicological impact of pharmaceuticals found in treated wastewaters: study of carbamazepine, clofibric acid, and diclofenac. Ecotoxicol. Environ. Saf. 55, 359–370. https://doi.org/10.1016/S0147-6513(02)00082-9.
Flicek, P., Amode, M.R., Barrell, D., Beal, K., Brent, S., Carvalho-Silva, D., Clapham, P., Coates, G., Fairley, S., Fitzgerald, S., Gil, L., Gordon, L., Hendrix, M., Hourlier, T., Johnson, N., Kähäri, A.K., Keefe, D., Keenan, S., Kinsella, R., Komorowska, M., Koscielny, G., Kulesha, E., Larsson, P., Longden, I., McLaren, W., Muffato, M., Overduin, B., Pignatelli, M., Pritchard, B., Riat, H.S., Ritchie, G.R.S., Ruffier, M., Schuster, M., Sobral, D., Tang, Y.A., Taylor, K., Trevanion, S., Vandrovcova, J., White, S., Wilson, M., Wilder, S.P., Aken, B.L., Birney, E., Cunningham, F., Dunham, I., Durbin, R., Fernández-Suarez, X.M., Harrow, J., Herrero, J., Hubbard, T.J.P., Parker, A., Proctor, G., Spudich, G., Vogel, J., Yates, A., Zadissa, A., Searle, S.M.J., 2012. Ensembl 2012. Nucleic Acids Res, vol. 40, pp. D84–D90. https://doi.org/10.1093/nar/gkr991.
Garcia de la serrana, D., Wreggelsworth, K., Johnston, I.A., 2018. Duplication of a single myhz1.1 gene facilitated the ability of goldfish (Carassius auratus) to alter fast muscle contractile properties with seasonal temperature change. Front. Physiol. 9 https://doi.org/10.3389/fphys.2018.01724.
Gardiner, M.R., Gongora, M.M., Grimmond, S.M., Perkins, A.C., 2007. A global role for zebrafish klf4 in embryonic erythropoiesis. Mech. Dev. 124, 762–774. https://doi.org/10.1016/j.mod.2007.06.005.
Gunnarsson, L., Jauhiainen, A., Kristiansson, E., Nerman, O., Larsson, D.G.J., 2008. Evolutionary conservation of human drug targets in organisms used for environmental risk assessments. Environ. Sci. Technol. 42, 5807–5813. https://doi.org/10.1021/es8005173.
Haffter, P., Odenthal, J., Mullins, M.C., Lin, S., Farrell, M.J., Vogelsang, E., Haas, F., Brand, M., van Eeden, F.J.M., Furutani-Seiki, M., Granato, M., Hammerschmidt, M., Heisenberg, C.-P., Jiang, Y.-J., Kane, D.A., Kelsh, R.N., Hopkins, N., Nüsslein-Volhard, C., 1996. Mutations affecting pigmentation and shape of the adult zebrafish. Dev. Gene. Evol. 206, 260–276. https://doi.org/10.1007/s004270050051.
Hansen, C.G., Nichols, B.J., 2010. Exploring the caves: cavins, caveolins and caveolae. Trends Cell Biol. 20, 177–186. https://doi.org/10.1016/j.tcb.2010.01.005.
Heffer, A., Marquart, G.D., Aquilina-Beck, A., Saleem, N., Burgess, H.A., Dawid, I.B., 2017. Generation and characterization of Kctd15 mutations in zebrafish. PloS One 12, e0189162. https://doi.org/10.1371/journal.pone.0189162.
Hellemans, J., Mortier, G., De Paepe, A., Speleman, F., Vandesompele, J., 2007. qBase relative quantification framework and software for management and automated analysis of real-time quantitative PCR data. Genome Biol. 8, R19. https://doi.org/10.1186/gb-2007-8-2-r19.
Hermsen, S.A.B., Pronk, T.E., van den Brandhof, E.-J., van der Ven, L.T.M., Piersma, A.H., 2013. Transcriptomic analysis in the developing zebrafish embryo after compound exposure: individual gene expression and pathway regulation. Toxicol. Appl. Pharmacol. 272, 161–171. https://doi.org/10.1016/j.taap.2013.05.037.
Howe, D.G., Bradford, Y.M., Conlin, T., Eagle, A.E., Fashena, D., Frazer, K., Knight, J., Mani, P., Martin, R., Moxon, S.A.T., Paddock, H., Pich, C., Ramachandran, S., Ruef, B.J., Ruzicka, L., Schaper, K., Shao, X., Singer, A., Sprunger, B., Van Slyke, C.E., Westerfield, M., 2013. ZFIN, the Zebrafish Model Organism Database: increased support for mutants and transgenics. Nucleic Acids Res. 41, D854–D860. https://doi.org/10.1093/nar/gks938.
Hsu, S.-C., Chang, Y.-T., Chen, C.-C., 2013. Early growth response 1 is an early signal inducing Cav 3.2 T-type calcium channels during cardiac hypertrophy. Cardiovasc. Res. 100, 222–230. https://doi.org/10.1093/cvr/cvt190.
Hughes, S.R., Kay, P., Brown, L.E., 2013. Global synthesis and critical evaluation of pharmaceutical data sets collected from river systems. Environ. Sci. Technol. 47, 661–677. https://doi.org/10.1021/es3030148.
Incardona, J.P., Scholz, N.L., 2017. 6 - environmental pollution and the fish heart. In: Gamperl, A.K., Gillis, T.E., Farrell, A.P., Brauner, C.J. (Eds.), Fish Physiology, the Cardiovascular System. Academic Press, pp. 373–433. https://doi.org/10.1016/bs.fp.2017.09.006.
Incardona, J.P., Scholz, N.L., 2016. The influence of heart developmental anatomy on cardiotoxicity-based adverse outcome pathways in fish. Aquat. Toxicol. 177, 515–525. https://doi.org/10.1016/j.aquatox.2016.06.016.
Jao, L.-E., Wente, S.R., Chen, W., 2013. Efficient multiplex biallelic zebrafish genome editing using a CRISPR nuclease system. Proc. Natl. Acad. Sci. Unit. States Am.

110, 13904–13909. https://doi.org/10.1073/pnas.1308335110.
Kelsh, R.N., Schmid, B., Eisen, J.S., 2000. Genetic analysis of melanophore development in zebrafish embryos. Dev. Biol. 225, 277–293. https://doi.org/10.1006/dbio.2000.9840.
Koutnikova, H., Laakso, M., Lu, L., Combe, R., Paananen, J., Kuulasmaa, T., Kuusisto, J., Häring, H.-U., Hansen, T., Pedersen, O., Smith, U., Hanefeld, M., Williams, R.W., Auwerx, J., 2009. Identification of the UBP1 locus as a critical blood pressure determinant using a combination of mouse and human genetics. PLoS Genet. 5, e1000591 https://doi.org/10.1371/journal.pgen.1000591.
Kramer-Zucker, A.G., Wiessner, S., Jensen, A.M., Drummond, I.A., 2005. Organization of the pronephric filtration apparatus in zebrafish requires Nephrin, Podocin and the FERM domain protein Mosaic eyes. Dev. Biol. 285, 316–329. https://doi.org/10.1016/j.ydbio.2005.06.038.
Kubista, M., Andrade, J.M., Bengtsson, M., Forootan, A., Jonák, J., Lind, K., Sindelka, R., Sjöback, R., Sjögreen, B., Strömbom, L., Ståhlberg, A., Zoric, N., 2006. The real-time polymerase chain reaction. Mol. Aspect. Med. 27, 95–125. https://doi.org/10.1016/j.mam.2005.12.007.
LaLone, C.A., Ankley, G.T., Belanger, S.E., Embry, M.R., Hodges, G., Knapen, D., Munn, S., Perkins, E.J., Rudd, M.A., Villeneuve, D.L., Whelan, M., Willett, C., Zhang, X., Hecker, M., 2017. Advancing the adverse outcome pathway framework—an international horizon scanning approach. Environ. Toxicol. Chem. 36, 1411–1421. https://doi.org/10.1002/etc.3805.
Lamason, R.L., Mohideen, M.-A.P.K., Mest, J.R., Wong, A.C., Norton, H.L., Aros, M.C., Jurynec, M.J., Mao, X., Humphreville, V.R., Humbert, J.E., Sinha, S., Moore, J.L., Jagadeeswaran, P., Zhao, W., Ning, G., Makalowska, I., McKeigue, P.M., O'Donnell, D., Kittles, R., Parra, E.J., Mangini, N.J., Grunwald, D.J., Shriver, M.D., Canfield, V.A., Cheng, K.C., 2005. SLC24A5, a putative cation exchanger, affects pigmentation in zebrafish and humans. Science 310, 1782–1786. https://doi.org/10.1126/science.1116238.
Lee, Y., Gunten, U. von, 2016. Advances in predicting organic contaminant abatement during ozonation of municipal wastewater effluent: reaction kinetics, transformation products, and changes of biological effects. Environ. Sci. Water Res. Technol. 2, 421–442. https://doi.org/10.1039/C6EW00025H.
Lister, J.A., Lane, B.M., Nguyen, A., Lunney, K., 2011. Embryonic expression of zebrafish MiT family genes tfe3b, tfeb, and tfec. Dev. Dynam. 240, 2529–2538. https://doi.org/10.1002/dvdy.22743.
Liu, R., Zhang, W., Liu, Z.-Q., Zhou, H.-H., 2017. Associating transcriptional modules with colon cancer survival through weighted gene co-expression network analysis. BMC Genom. 18, 1–9. https://doi.org/10.1186/s12864-017-3761-z.
Lo, H.P., Nixon, S.J., Hall, T.E., Cowling, B.S., Ferguson, C., Morgan, G.P., Schieber, N.L., Fernandez-Rojo, M.A., Bastiani, M., Floetenmeyer, M., Martel, N., Laporte, J., Pilch, P.F., Parton, R.G., 2015. The caveolin–cavin system plays a conserved and critical role in mechanoprotection of skeletal muscle. J. Cell Biol. 210, 833–849. https://doi.org/10.1083/jcb.201501046.
Luo, Y., Guo, W., Ngo, H.H., Nghiem, L.D., Hai, F.I., Zhang, J., Liang, S., Wang, X.C., 2014. A review on the occurrence of micropollutants in the aquatic environment and their fate and removal during wastewater treatment. Sci. Total Environ. 473–474, 619–641. https://doi.org/10.1016/j.scitotenv.2013.12.065.
Mahony, C.B., Fish, R.J., Pasche, C., Bertrand, J.Y., 2016. Tfec controls the hematopoietic stem cell vascular niche during zebrafish embryogenesis. Blood 128, 1336–1345. https://doi.org/10.1182/blood-2016-04-710137.
Mahony, S., Benos, P.V., 2007. STAMP: a web tool for exploring DNA-binding motif similarities. Nucleic Acids Res. 35, W253–W258. https://doi.org/10.1093/nar/gkm272.
Manohar, M., Mei, H., Franklin, A.J., Sweet, E.M., Shigaki, T., Riley, B.B., MacDiarmid, C.W., Hirschi, K., 2010. Zebrafish (Danio rerio) endomembrane antiporter similar to a yeast cation/H+ transporter is required for neural crest development. Biochemistry 49, 6557–6566. https://doi.org/10.1021/bi100362k.
Matys, V., Fricke, E., Geffers, R., Gössling, E., Haubrock, M., Hehl, R., Hornischer, K., Karas, D., Kel, A.E., Kel-Margoulis, O.V., Kloos, D.-U., Land, S., Lewicki-Potapov, B., Michael, H., Münch, R., Reuter, I., Rotert, S., Saxel, H., Scheer, M., Thiele, S., Wingender, E., 2003. TRANSFAC: transcriptional regulation, from patterns to profiles. Nucleic Acids Res. 31, 374–378. https://doi.org/10.1093/nar/gkg108.
Meng, Q., Yeung, K., Kwok, M.L., Chung, C.T., Hu, X.L., Chan, K.M., 2020. Toxic effects and transcriptome analyses of zebrafish (Danio rerio) larvae exposed to benzophenones. Environ. Pollut. 265, 114857. https://doi.org/10.1016/j.envpol.2020.114857.
Naito, D., Ogata, T., Hamaoka, T., Nakanishi, N., Miyagawa, K., Maruyama, N., Kasahara, T., Taniguchi, T., Nishi, M., Matoba, S., Ueyama, T., 2015. The coiled-coil domain of MURC/cavin-4 is involved in membrane trafficking of caveolin-3 in cardiomyocytes. Am. J. Physiol. Heart Circ. Physiol. 309, H2127–H2136. https://doi.org/10.1152/ajpheart.00446.2015.
Neidhardt, J., Fehr, S., Kutsche, M., Löhler, J., Schachner, M., 2003. Tenascin-N: characterization of a novel member of the tenascin family that mediates neurite repulsion from hippocampal explants. Mol. Cell. Neurosci. 23, 193–209. https://doi.org/10.1016/S1044-7431(03)00012-5.
Obayashi, T., Kagaya, Y., Aoki, Y., Tadaka, S., Kinoshita, K., 2019. COXPRESdb v7: a gene coexpression database for 11 animal species supported by 23 coexpression platforms for technical evaluation and evolutionary inference. Nucleic Acids Res. 47, D55–D62. https://doi.org/10.1093/nar/gky1155.
Ogata, T., Ueyama, T., Isodono, K., Tagawa, M., Takehara, N., Kawashima, T., Harada, K., Takahashi, T., Shioi, T., Matsubara, H., Oh, H., 2008. MURC, a muscle-restricted coiled-coil protein that modulates the rho/ROCK pathway, induces cardiac dysfunction and conduction disturbance. Mol. Cell Biol. 28, 3424–3436. https://doi.org/10.1128/MCB.02186-07.
Ojehomon, M., Alderman, S.L., Sandhu, L., Sutcliffe, S., Van Raay, T., Gillis, T.E., Dawson, J.F., 2018. Identification of the actc1c cardiac actin gene in zebrafish. Prog. Biophys. Mol. Biol., The Use of Zebrafish for Card. Res. 138, 32–37. https://doi.org/10.1016/j.pbiomolbio.2018.06.007.
Park, J.-S., Ryu, J.-H., Choi, T.-I., Bae, Y.-K., Lee, S., Kang, H.J., Kim, C.-H., 2016. Innate color preference of zebrafish and its use in behavioral analyses. Moleucles Cells 39, 750–755. https://doi.org/10.14348/molcells.2016.0173.
Petratou, K., Spencer, S.A., Kelsh, R.N., Lister, J.A., 2019. The MITF Paralog Tfec Is Required in Neural Crest Development for Fate Specification of the Iridophore Lineage from a Multipotent Pigment Cell Progenitor. https://doi.org/10.1101/862011 bioRxiv 862011.
Pfaffl, M.W., 2001. A new mathematical model for relative quantification in real-time RT-PCR. Nucleic Acids Res. 29, e45. https://doi.org/10.1093/nar/29.9.e45.
Pfaffl, M.W., Tichopad, A., Prgomet, C., Neuvians, T.P., 2004. Determination of stable housekeeping genes, differentially regulated target genes and sample integrity: BestKeeper – excel-based tool using pair-wise correlations. Biotechnol. Lett. 26, 509–515. https://doi.org/10.1023/B:BILE.0000019559.84305.47.
Pohl, J., Ahrens, L., Carlsson, G., Golovko, O., Norrgren, L., Weiss, J., Örn, S., 2019. Embryotoxicity of ozonated diclofenac, carbamazepine, and oxazepam in zebrafish (Danio rerio). Chemosphere 225, 191–199. https://doi.org/10.1016/j.chemosphere.2019.03.034.
Pohl, J., Golovko, O., Carlsson, G., Eriksson, J., Glynn, A., Örn, S., Weiss, J., 2020. Carbamazepine ozonation byproducts: toxicity in zebrafish (*Danio rerio*) embryos and chemical stability. Environ. Sci. Technol. 54, 2913–2921. https://doi.org/10.1021/acs.est.9b07100.
Potterf, S.B., Mollaaghababa, R., Hou, L., Southard-Smith, E.M., Hornyak, T.J., Arnheiter, H., Pavan, W.J., 2001. Analysis of SOX10 function in neural crest-derived melanocyte development: SOX10-dependent transcriptional control of dopachrome tautomerase. Dev. Biol. 237, 245–257. https://doi.org/10.1006/dbio.2001.0372.
Qiang, L., Cheng, J., Yi, J., Rotchell, J.M., Zhu, X., Zhou, J., 2016. Environmental concentration of carbamazepine accelerates fish embryonic development and disturbs larvae behavior. Ecotoxicology 25, 1426–1437. https://doi.org/10.1007/s10646-016-1694-y.
R Core Team, 2019. R: A Language and Environment for Statistical Computing. R Foundation for Statistical Computing, Vienna, Austria.
Rehli, M., Den Elzen, N., Cassady, A.I., Ostrowski, M.C., Hume, D.A., 1999. Cloning and characterization of the murine genes for bHLH-ZIP transcription factors TFEC and TFEB reveal a common gene organization for all MiT subfamily members. Genomics 56, 111–120. https://doi.org/10.1006/geno.1998.5588.
RStudio Team, 2020. RStudio. Integrated Development for R. RStudio PBC, Boston MA.
Scherberich, A., Tucker, R.P., Samandari, E., Brown-Luedi, M., Martin, D., Chiquet-Ehrismann, R., 2004. Murine tenascin-W: a novel mammalian tenascin expressed in kidney and at sites of bone and smooth muscle development. J. Cell Sci. 117, 571–581. https://doi.org/10.1242/jcs.00867.
Serra, A., Fratello, M., Cattelani, L., Liampa, I., Melagraki, G., Kohonen, P., Nymark, P., Federico, A., Kinaret, P.A.S., Jagiello, K., Ha, M.K., Choi, J.-S., Sanabria, N., Gulumian, M., Puzyn, T., Yoon, T.-H., Sarimveis, H., Grafström, R., Afantitis, A., Greco, D., 2020. Transcriptomics in toxicogenomics, Part III: data modelling for risk assessment. Nanomaterials 10, 708. https://doi.org/10.3390/nano10040708.
Shen, J., Xing, W., Gong, F., Wang, W., Yan, Y., Zhang, Y., Xie, C., Fu, S., 2019. MiR-150-5p retards the progression of myocardial fibrosis by targeting EGR1. Cell Cycle 18, 1335–1348. https://doi.org/10.1080/15384101.2019.1617614.
Shih, Y.-H., Zhang, Y., Ding, Y., Ross, C.A., Li, H., Olson, T.M., Xu, X., 2015. Cardiac transcriptome and dilated cardiomyopathy genes in zebrafish. Circ. Cardiovasc. Genet. 8, 261–269. https://doi.org/10.1161/CIRCGENETICS.114.000702.
Shorvon, S., Perucca, E., Engel Jr., J., 2017. The Treatment of Epilepsy, fourth ed., vol. 2017. Wiley. 2017.
Sogah, V.M., Serluca, F.C., Fishman, M.C., Yelon, D.L., MacRae, C.A., Mably, J.D., 2010. Distinct troponin C isoform requirements in cardiac and skeletal muscle. Dev. Dynam. 239, 3115–3123. https://doi.org/10.1002/dvdy.22445.
Thisse, B., Thisse, C., 2004. Fast Release Clones: A High Throughput Expression Analysis. ZFIN Direct Data Submiss. Httpzfinorg.
van Dam, S., Võsa, U., van der Graaf, A., Franke, L., de Magalhães, J.P., 2018. Gene co-expression analysis for functional classification and gene–disease predictions. Briefings Bioinf. 19, 575–592. https://doi.org/10.1093/bib/bbw139.
Vandesompele, J., De Preter, K., Pattyn, F., Poppe, B., Van Roy, N., De Paepe, A., Speleman, F., 2002. Accurate normalization of real-time quantitative RT-PCR data by geometric averaging of multiple internal control genes. Genome Biol. 3 https://doi.org/10.1186/gb-2002-3-7-research0034 research0034.1.
Villeneuve, D., Volz, D.C., Embry, M.R., Ankley, G.T., Belanger, S.E., Léonard, M., Schirmer, K., Tanguay, R., Truong, L., Wehmas, L., 2014. Investigating Alternatives to the fish early-life stage test: a strategy for discovering and annotating adverse outcome pathways for early fish development. Environ. Toxicol. Chem. 33, 158–169. https://doi.org/10.1002/etc.2403.
Winata, C.L., Korzh, S., Kondrychyn, I., Korzh, V., Gong, Z., 2010. The role of vasculature and blood circulation in zebrafish swimbladder development. BMC Dev. Biol. 10, 1–9. https://doi.org/10.1186/1471-213X-10-3.
Winata, C.L., Korzh, S., Kondrychyn, I., Zheng, W., Korzh, V., Gong, Z., 2009. Development of zebrafish swimbladder: the requirement of Hedgehog signaling in specification and organization of the three tissue layers. Dev. Biol. 331, 222–236. https://doi.org/10.1016/j.ydbio.2009.04.035.
Yan, S., Wang, M., Zha, J., Zhu, L., Li, W., Luo, Q., Sun, J., Wang, Z., 2018.

Environmentally relevant concentrations of carbamazepine caused endocrine-disrupting effects on nontarget organisms, Chinese rare minnows (*Gobiocypris rarus*). Environ. Sci. Technol. 52, 886–894. https://doi.org/10.1021/acs.est.7b06476.

Yang, Y., Han, L., Yuan, Y., Li, J., Hei, N., Liang, H., 2014. Gene co-expression network analysis reveals common system-level properties of prognostic genes across cancer types. Nat. Commun. 5, 3231. https://doi.org/10.1038/ncomms4231.

Yoshida, T., Gan, Q., Franke, A.S., Ho, R., Zhang, J., Chen, Y.E., Hayashi, M., Majesky, M.W., Somlyo, A.V., Owens, G.K., 2010. Smooth and cardiac muscle-selective knock-out of krüppel-like factor 4 causes postnatal death and growth retardation. J. Biol. Chem. 285, 21175–21184. https://doi.org/10.1074/jbc.M110.112482.

Yousaf, S., Sethna, S., Chaudhary, M.A., Shaikh, R.S., Riazuddin, S., Ahmed, Z.M., 2020. Molecular characterization of SLC24A5 variants and evaluation of Nitisinone treatment efficacy in a zebrafish model of OCA6. Pigment Cell Melanoma Res 33, 556–565. https://doi.org/10.1111/pcmr.12879.

Zhang, S., Ng, M.K., 2016. Gene-microRNA network module analysis for ovarian cancer. BMC Syst. Biol. 10, 445–455. https://doi.org/10.1186/s12918-016-0357-1.